

Flux pinning allowing levitation experiments at liquid oxygen temperature

M. Muralidhar^{1*}, N. Sakai¹, M. Jirsa^{1,2}, M. Murakami^{1,3} & N. Koshizuka¹

¹Superconductivity Research Laboratory (SRL), ISTEC, 3-35-2, Lioka-Shinden, Morioka, Iwate 020-0852, JAPAN

*Fax:+81-19-635-9017, e-mail: miryala1@istec.or.jp

²Institute of Physics, ASCR, CZ-182 21 Praha 8, Czech Republic

³Shibaura Institute of Technology, Shibaura 3-9-14, Minato-Ku, Tokyo 108-8548, JAPAN

A new type of (Nd,Eu,Gd)Ba₂Cu₃O_y “NEG-123” composite with exceptionally small secondary phase particles exhibits a high flux pinning up to a close vicinity of T_c . The externally added ball-milled secondary phase particles partially transformed during the technological process to a new type of nanometer-scale Zr-rich secondary phase pins. The critical current density improved in high temperatures by an order of magnitude as compared to other RE-123 type materials. Analysis of the normalized pinning force versus reduced field for various amounts of Zr-rich particles implies a potential role of ΔT_c pinning. The exceptionally good pinning performance led to realization of a levitation experiment with a permanent magnet suspended over and below the NEG-123 superconductor cooled by liquid oxygen. The new type of bulk superconducting magnets may serve as construction materials for liquid oxygen pumps in various applications.

Key words: melt-textured, micro-structure, critical current density, flux pinning, levitation at 90 K

1. INTRODUCTION

The old dream to utilize bulk high- T_c superconducting magnets at liquid oxygen temperature has recently become much more feasible due to the progress in fabrication of NEG-123 materials [1]. Although YBa₂Cu₃O “Y-123”, commonly used for levitation at 77 K, has critical temperature (91-93 K) [2], lying only slightly below that of NEG-123, the pinning performance of Y-123 rapidly drops at high temperatures and therefore is insufficient for levitation at 90 K. Even worse situation is met by the superconductors with T_c above 100 K [3, 4], like Bi-Sr-Ca-Cu-O, Tl-Ba-Cu-O and others. These compounds cannot be used for levitation even with liquid nitrogen cooling. At present only the new NEG-123 composite exhibits a sufficiently good pinning performance up to temperatures above 90 K.

Nd, Eu, and Gd are, together with Sm, are called light rare earths, “LRE”. The principle difference between Y-123 and NEG-123 is that LRE forms a solid solution with barium and the extent of this has to be regulated by reduction of oxygen in the melt-texturing process. One of such procedures is called the oxygen controlled melt growth “OCMG” process [5]. The OCMG LRE-123 materials exhibit T_c between 93 K and 96 K. However, up to recent the pinning performance of these materials also rapidly decreased above 80 K.

In mixed LRE-123 systems two principal classes of pinning defects coexist. One is the LRE/Ba substitution in the form of nanometer-scale clusters [6], resulting in an enhanced super-current densities at intermediate and high fields (secondary peak). The other one are rather large (micron and sub-micron scale) insulating LRE₂BaCuO₅ “LRE-211” or Nd₄Ba₂Cu₂O₁₀ “Nd-422” (in the case of LRE=Nd) particles embedded in the superconducting LRE-123 matrix [8, 9]. Each of these defect types is active in another field range and their performance can be optimized according to demands of a particular application. It is well known that the secondary phase particles are mainly active at low fields and

their pinning efficiency is inversely proportional to their dimension. Thus, in order to enhance critical currents at high temperatures, where the operating field range is strongly reduced, one should optimize the pinning by secondary phase particles. In attempt to do so, we gradually reduced the starting Gd-211 particle size by Y₂O₃ – ZrO₃ ball milling.

In this study, we examined two sets of samples. In the first set the amount of Gd-211 was fixed and the initially added particle size varied from 200 nm to 70 nm. In the second set, the Gd-211 secondary phase particle size was kept constant and the amount of Gd-211 was varied.

2. EXPERIMENTAL

In this work, we gradually reduced the size of starting Gd-211 particles added to (Nd_{0.33}Eu_{0.33}Gd_{0.33})Ba₂Cu₃O_y. The NEG-123 was produced in a routine way described e.g. in [5]. The Gd-211 powder was milled using Y₂O₃ – ZrO₃ balls in acetone, for 0.3, 2, 4, and 8 h. The average size of the ball-milled particles was 200 – <70 nm, in dependence of the milling time. The size was estimated by Brunauer-Emmerit-Teller (BET) specific area measurements [10]. 10 to 50 mol% of the ball-milled Gd-211 were added to the sintered NEG-123. For suppression of Gd-211 particles coarsening during melt processing, 0.5 mol% Pt and 1 mol% CeO₂ were added. The pellets were grown by OCMG process in Ar with 1% partial pressure of O₂. For magnetic measurements, small specimens with dimensions of $a \times b \times c \approx 1.5 \times 1.5 \times 0.5$ mm³ were cut from the pellets and annealed in flowing oxygen in the temperature range 300-600 °C [5].

The microstructure of these samples was studied with a scanning electron microscope “SEM”, a dynamic force microscope “DFM” and a transmission electron microscope “TEM”. Magnetization hysteresis loops “*M-H* loops” were measured at 77 K using a commercial SQUID magnetometer (Quantum Design, model MPMS7) in field range –2 to +7 T. To minimize field inhomogeneity, the scan length was

restricted to 1 cm. The external magnetic field was applied parallel to the c -axis of the samples. J_c values were estimated from the M - H loops using the extended Bean critical state formula for a rectangular sample [11]. Magnetization characterization was performed by measuring hysteresis loops and analyzing the normalized volume pinning forces, F_p , as a function of reduced field $h = H_d/H_{irr}$.

3. EXPERIMENTAL RESULTS

Morphology of the resulting secondary phase network in the NEG-123 matrix was studied by scanning electron microscopy on several samples with various Gd-211 initial particle sizes. Figure 1 (a) shows SEM image of the NEG-123 sample with 30 mol% Gd-211 (70 nm).

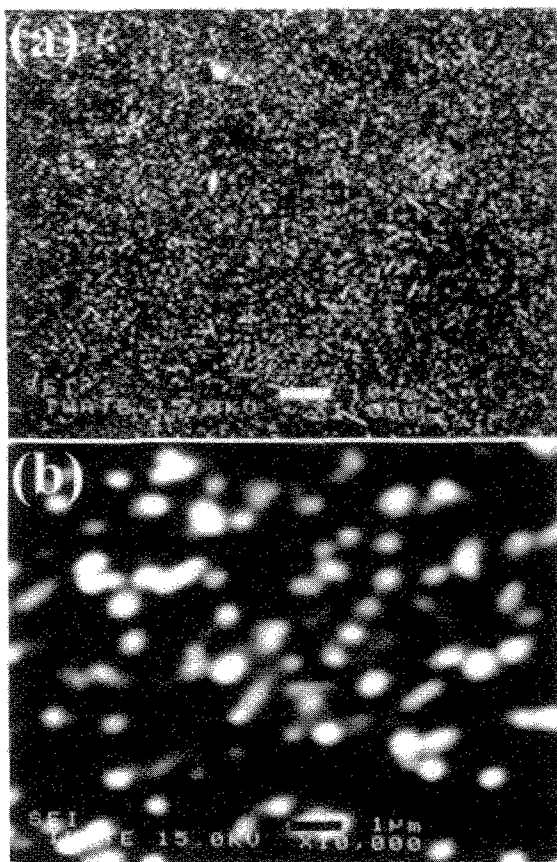


Fig.1 Scanning electron micrographs of NEG-123 + 30 mol% Gd-211 (average particle size is 70 nm) prepared under 1% partial pressure of O_2 : (a) low magnification scanning electron micrograph, (b) high magnification scanning electron micrograph. Note that fine 211 inclusions with the size ranging from 300 to 500 nm are uniformly dispersed in the matrix.

A notable feature is the uniformity of the secondary phase particles dispersion. SEM image taken at a higher magnification (Fig. 1(b)) showed particles ranging between 200 to 500 nm, larger than the original size. To acquire better insight and resolution, a TEM study was made on the same sample (Figure 2). Two types of defects can be seen: large irregular inclusions of about 200 to 500 nm in size as observed in Figure 1 (b) and round particles of 20-50 nm

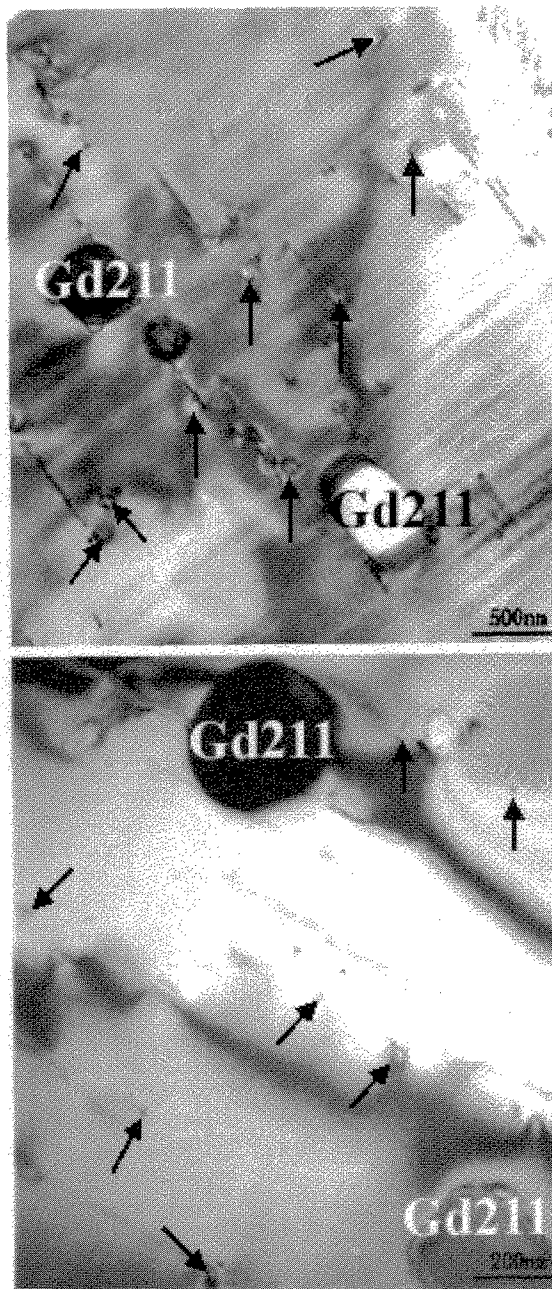


Fig. 2. Transmission electron micrograph of NEG-123 sample with 30 mol% Gd-211 (average particle size is 70 nm); the black arrows show some nanometer size Zr-rich particles.

size. The chemical identification of the precipitates was made by scanning TEM-EDX analysis. The analyzed spot of 2-3 nm in diameter enabled to unambiguously analyze even the smallest clusters. More than 65 nanoparticles were studied. The quantitative analysis clarified that the large particles are Gd-211/Gd-rich-NEG-211, which is in agreement with our earlier studies of the NEG-123 system [8]. In contrast, the small defects with size below 50 nm always contained a significant amount of Zr. These defects

are marked in Fig. 2 by arrows. A similar feature was observed on different parts of the sample. As no zirconium was intentionally introduced into the sample, we concluded that the Zr contaminated the secondary phase powders during the ball-milling process and specifically affected the particle size reduction during the melt-growth process. This result was also confirmed by dynamic force microscopy. More details of nanometer size Zr-rich pinning centers and their chemical analyses can be found in Ref. [12].

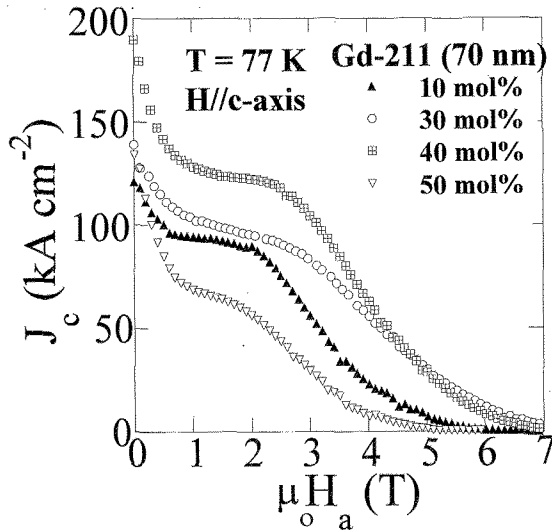


Fig. 3. Field dependence of J_c for NEG-123 samples with 10 to 50 mol% Gd-211 refined by ball-milling for 4 h (70 nm). All the samples were measured at $T = 77$ K for $H//c$ -axis. The current density increased in the whole field range with increasing content of the secondary phase up to 40 mol% but dropped above this content. Record critical current densities of 194 and 110 kA/cm^2 were achieved at 0 and 3 T, respectively.

Fig. 3 shows the field dependence of the critical current density, J_c , for NEG-123 samples with the Gd-211 content ranging between 10 and 50 mol%. The $J_c(H)$ curves were deduced from SQUID magnetometer measurements at 77 K in applied field parallel to the c -axis. In all the samples, the initial average secondary particle size was 70 nm. It is evident that the critical current density both at low and high magnetic fields depends on the amount of initially added secondary phase. The sample with 40 mol% Gd-211 showed the remnant J_c value around 194 kA/cm^2 and 110 kA/cm^2 at 3 T. This result is by more than 60% higher than the previous record value of NEG-123 and by more than an order of magnitude higher than those in other RE-123 materials. With further increase of the Gd-211 content to 50 mol% the critical current density decreased. This may be due to the excessive Zr contamination of the Gd-211 secondary phase [13].

In order to study the role of initially added secondary phase size, the Gd-211 content was kept constant at 30 mol% and the starting average particle size was varied between 200 nm and <70 nm. The field dependence of critical current density at 77 K and $H//c$ -axis are shown in Figure 4. A clear increase of the remnant J_c with decreasing the particles size is visible. Remarkable is the record value of the remnant J_c , 190 kA/cm^2 , reached with the average starting particle size

of <70 nm. Another important feature is that the high-field pinning systematically improved with decreasing the particle size.

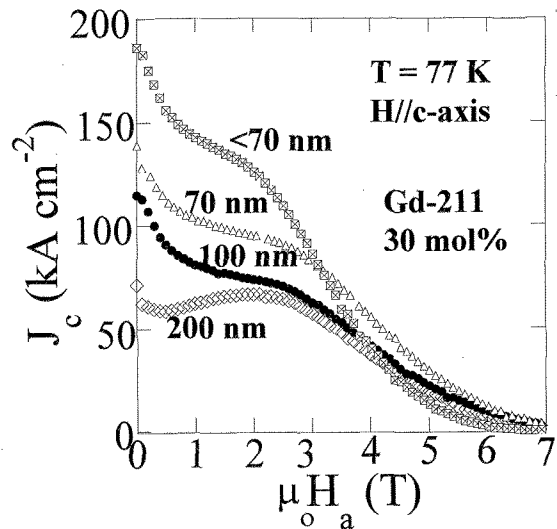


Fig. 4. Field dependence of critical current density for NEG-123 samples with 30 mol% Gd-211 refined by ball-milling for 0.3, 2, 4 h, and 8 h (200 nm, 100 nm, 70 nm, <70 nm). All the samples were measured at $T = 77$ K for $H//c$ -axis. The current density increased in the whole field range with decreasing particle size. High critical current densities of 190 and 100 kA/cm^2 were achieved at 0 and 3 T, respectively.

The pinning performance of the Gd-211 phase contaminated by Zr was studied by using the normalized volume pinning force density, $F_p = BJ_c / (B_{\text{max}} J_{c\text{max}})$, as a function of the reduced field, $h = H_a / H_{\text{irr}}$, where B_{max} and $J_{c\text{max}}$ are the magnetic induction and J_c values at the secondary peak maximum, H_a is the applied field, and H_{irr} is the irreversibility field. The $F_p(h)$ curves for three NEG-123 samples with different initial Gd-211 particle sizes, nicely scaled in a temperature range of 70 - 90 K, are shown in Figure 5. In the top and middle graphs $F_p(h)$ curves of the samples with 30 mol% Gd-211 of the initial size 200 and 70 nm are presented, respectively. H_{irr} was derived from magnetization hysteresis loops using the criterion of 100 A/cm^2 . It was found that the peak on the $F_p(h)$ curves for both samples lies around $h = 0.50$, only for the Gd-211 size < 70 nm (bottom figure) the peak position slightly shifted to lower fields, $h = 0.43$. Such a relatively high position of the secondary peak was theoretically predicted for ΔT_c pinning [14]. However, the pinning mechanism associated with the secondary peak has not yet been unambiguously identified.

The magnetic study and the microstructure analysis indicate that for the observed improvement of the flux pinning performance of the NEG-123 compound a combination of nanometer-sized Gd-211 particles with the extremely small Zr-rich clusters is the base.

The pinning enhancement due to a new type of defects is so profound that it extends up to temperatures above 90 K (see Fig. 6). This means that the limiting operating temperature for levitation experiments and other applications shifts from liquid nitrogen (77.3 K) to liquid oxygen (90.2 K). This is documented in Fig. 7 (a) where we a conventional levitation experiment with a permanent Fe-Nd-B magnet levitating

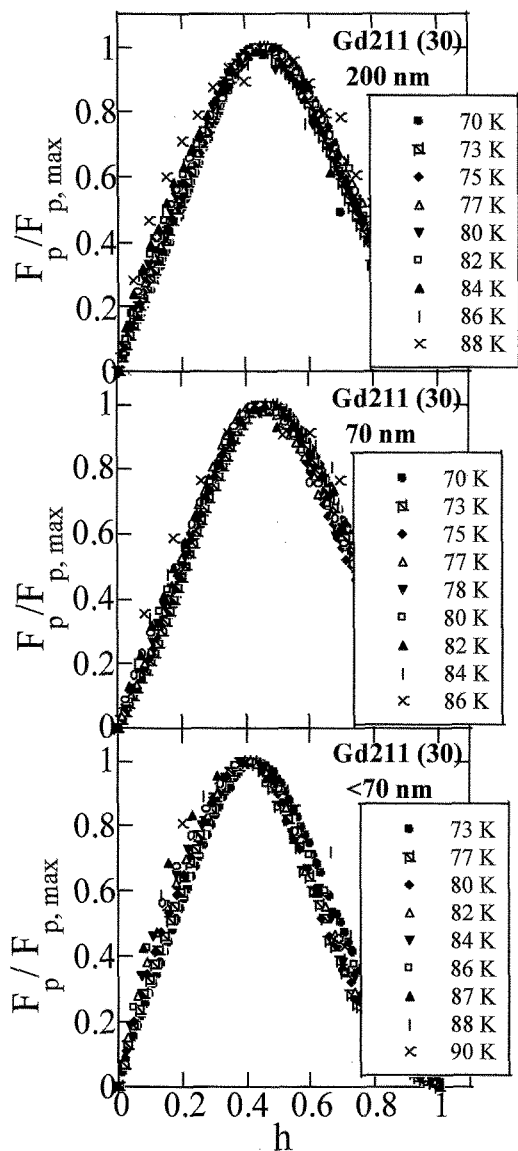


Fig. 5. Scaling of the normalized pinning forces, $F_p/F_{p,max}$, vs reduced field, $h=H_a/H_{im}$, for NEG-123 + 30 mol% Gd-211 with 200 nm (top), 70 nm (middle) and < 70 nm (bottom) particles at temperatures between 70 and 90 K. The scaling with temperature is very good, the curve peaks at $h \approx 0.5$ for 200 and 70 nm and at 0.43 for < 70 nm.

above the NEG-123 sample with 40 mol% Gd-211 immersed in liquid oxygen. Fig. 7 (b) presents an alternative experiment, levitation of two *superconducting* magnets. In this case, the upper magnet was first magnetized at 90 K in a uniform external field of 0.5 T. Then it was put in a close distance to the same material and these were field-cooled to 90 K in stray field of the upper magnet. After removal of the spacing, the first NEG-123 magnet “hanged” in the potential well formed by the stray field trapped in the lower superconductor. After magnetization process the system was taken out of liquid oxygen. As a result, one NEG-123

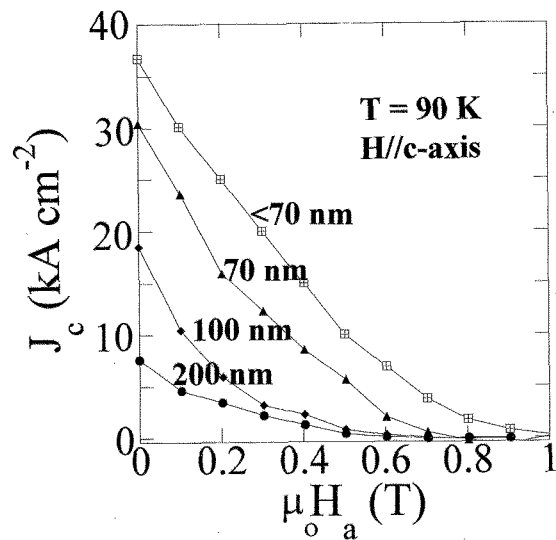


Fig. 6. Field dependence of J_c for NEG-123 samples with 30 mol% Gd-211 refined by ball-milling for 0.3, 2, 4, and 8h (200, 100, 70, and <70 nm). All the samples were measured at $T=90$ K with $H//c$ -axis. A critical current density is still high at liquid oxygen temperature, 90 K.

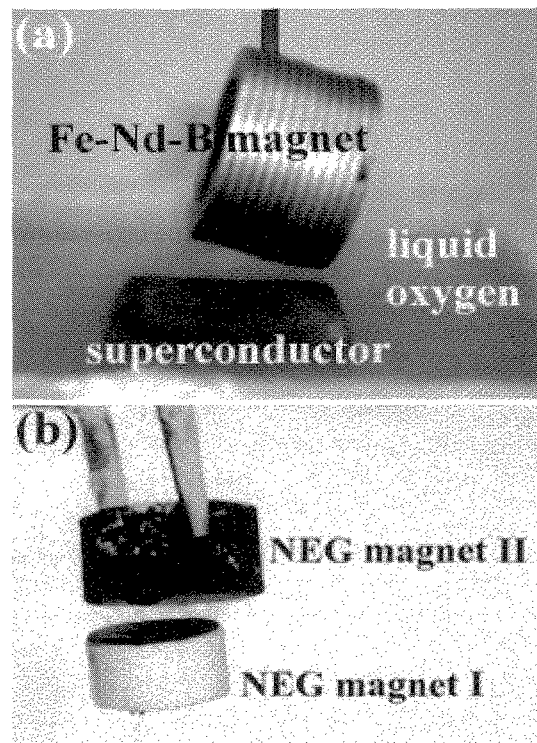


Fig. 7. (a) Permanent Fe-Nd-B magnet levitating over an NEG-123 + 40 mol% Gd-211 (average particle size 70 nm) superconductor at liquid oxygen temperature (90 K), after the superconductor had been magnetized by stray field of the permanent magnet and cooled down to 90 K; (b) NEG-123 pellet suspended below another NEG-123 “permanent” magnet.

magnet hanged *below* the second one. These achievements will promote the development of novel applications in medical and space programs.

Today's hospital requires comprehensive medical gas distribution systems to meet increasing demands of the life support technologies and emergency help. Medical gases have to be distributed in a clean, safe, and reliable manner. Gases in liquid form can be transported in a sophisticated network, which would supply either medical air and/or oxygen for patient breathing support or nitrous oxide for anesthesia. For such systems, the new superconductors represent a basic construction material for design of non-contact liquid oxygen pumps.

4. SUMMARY

We showed that bulk NEG-123 materials with a reduced size of Gd-211 particles and the new nanometer-size Zr-rich secondary phase clusters exhibit an excellent electromagnetic performance. The enhanced pinning enabled levitation experiments in liquid oxygen. The employment of the new NEG-123 superconducting permanent magnets that function at liquid oxygen temperature will lead to novel applications.

Acknowledgements

This work was supported by the New Energy and Industrial Technology Development Organization (NEDO) as Collaborative Research and Development of Fundamental Technologies for Superconductivity Applications.

References

- [1] M. Muralidhar, N. Sakai, M. Jirsa, M. Murakami, & N. Koshizuka, *Supercond. Sci. Technol.* **16** at press (2003).
- [2] S. Jin, A. Fastnacht, T. H. Tiefel, R. C. Sherwood, *Phys. Rev. B.* **37**, 5828 (1988).
- [3] Z. Z. Sheng, A. M. Hermann, *Nature* **33**, 138 (1988).
- [4] H. Maeda, Y. Tanaka, M. Fukufomi, T. Asano, *Jpn. J. Appl. Phys.* **27**, L209 (1988).
- [5] M. Murakami, N. Sakai, T. Higuchi, S. I. Yoo, *Supercond. Sci. Technol.* **9**, 1015 (1996).
- [6] M. Muralidhar, M. Jirsa, N. Sakai, M. Murakami, *Appl. Phys. Lett.* **79**, 3107 (2001).
- [7] M. Muralidhar, N. Sakai, N. Chikumoto, M. Jirsa, T. Machi, M. Nishiyama, Y. Hu, M. Murakami *Phys. Rev. Letters* **89**, 2370011-1 (2002).
- [8] M. Muralidhar, M. R. Koblischka, P. Diko, M. Murakami, *Appl. Phys. Lett.* **76**, 91 (2000).
- [9] P. McGinn, W. Chen, N. Zhu, M. Lanagan, U. Balachandran, *Appl. Phys. Lett.* **57**, 1455 (1990).
- [10] S. Brunauer, P. H. Emmett, E. Teller, *J. Am. Chem. Soc.* **60**, 309 (1938).
- [11] D. X. Chen, R. B. Goldfarb, *J. Appl. Phys.* **66**, 2489 (1989).
- [12] M. Muralidhar, N. Sakai, M. Jirsa, M. Murakami, & N. Koshizuka, *Supercond. Sci. Technol.* at press (2003).
- [13] M. Muralidhar, N. Sakai, M. Jirsa, M. Murakami, & N. Koshizuka, *to be communicated* (2003).
- [14] D. Dew-Hughes, *Philos. Mag.* **30**, 293 (1974).

(Received October 13, 2003; Accepted March 5, 2004)